Cell Tissue Res (1997) 289:53–61

Cell & Tissue Research

Distribution of ionocytes in the saccular epithelium of the inner ear of two teleosts (*Oncorhynchus mykiss and Scophthalmus maximus)*

N. Mayer-Gostan[1], **H. Kossmann**[2], **A. Watrin**[1], **P. Payan**[3], **G. Boeuf**[2]

[1] Laboratoire de physiologie cellulaire et moléculaire, CNRS, UMR 6548, Université de Nice, Parc Valrose, Faculté des Sciences, F-06108 Nice Cedex 2, France
[2] IFREMER, Centre de Brest, Station Ressources Vivantes. BP 70, F-29280 Plouzané, France
[3] Laboratoire de physiologie et toxicologie environnementales, Université de Nice, Parc Valrose, Faculté des Sciences, F-06108 Nice Cedex 2, France

Received: 8 August 1996 / Accepted: 14 January 1997

Abstract. The saccular membranes of trout (*Oncorhynchus mykiss*) and turbot (*Scophthalmus maximus*) were examined to characterize specialized epithelial cells that might be responsible for ion exchange. The approach for localizing cell types was new for this tissue, as observations were made with a stereomicroscope and a light microscope in order to have a general view of the epithelium. No important differences between the two species were seen. The saccular tissue is a monolayer epithelium (except for the macula neural zone) surrounded by a layer of connective tissue invaded by many blood vessels. The use of the fluorescent probe DAPSMI and zinc iodide/osmium fixation-coloration defined two areas in which ionocytes were present. In the first, large ionocytes were grouped into a nearly complete, crowned meshwork around, but separated from, the macula. In the second area, opposite the macula, the ionocytes were smaller, cubical, and grouped in patches. Cells rich in Na^+, K^+-ATPase and carbonic anhydrase II were present in both areas. Contrary to previous studies in mammals and fish, ionocytes were also found in the epithelium of the saccule.

Key words: Ionocyte – Saccular epithelium – Inner ear – *Oncorhynchus mykiss, Scophthalmus maximus* (Teleostei)

Introduction

The inner ear of teleosts is not equipped with a structure similar to the cochlea, which characterizes higher vertebrates. The labyrinth of fish is involved in the maintenance of equilibrium and has nervous cells sensitive to pressure, movements and sound vibrations (Lowenstein 1971; Dale 1980). The membranous labyrinth of fish consists of three connecting chambers, viz. the utricle, saccule and lagena, each containing one otolith. These chambers also communicate with the three semi-circular canals, and the lumen of the entire system is filled with endolymph. Fish otoliths are calcium carbonate concretions with marked annual and daily rhythmic depositions (Panella 1971). Otolith microstructure is important as it reflects not only the age, but also the history of the somatic growth of the fish (Campana and Nielson 1985; Jones 1992).

The endolymph in the labyrinth of all vertebrates is characterized by high potassium. In mammals, the sodium concentration is low and thus the endolymph is an "intracellular-like" ionic medium for cations other than calcium (ionized calcium: 0.03 mM in the cochlear endolymph, 0.3 mM in the vestibular endolymph). Only a few studies have reported the composition of endolymph in fish and most deal with that in the saccule, because this chamber is the largest of the labyrinth in most species. Fish endolymph has a higher sodium concentration (110–140 mM: Enger 1964; Fänge et al. 1972; Watanabe and Miyamoto 1973; Mugiya and Takahashi 1985; Kalish 1991) than that (3–40 mM) in mammals (Sterkers et al. 1990). Another difference, described by Mugiya and Takahashi (1985), is that the saccular endolymph of fish is more alkaline than plasma (ΔpH 0.5–0.65 units), whereas endolymph and plasma have the same pH in mammals (Sterkers et al. 1990). Teleosts have no perilymph and the ionic composition of cranial fluids does not differ substantially from that of plasma (Enger 1964). In aerian vertebrates, the endolymph has always been found to be positive with respect to the perilymph, the voltage varying from +80 mV in the cochlea to +5 mV in the utricle (Sterkers et al. 1990). In teleosts, a saccular potential of about +10 mV has been reported (Enger 1964). This suggests that, in all cases, energy-dependent mechanisms maintain the K^+ concentration of

This study was supported by IFREMER (Programme: Régulation de la croissance chez les poissons). H. Kossmann was the recipient of a grant from the Ministère Français des Affaires Etrangères (programme ECOS CONICYT de coopération scientifique entre la France et le Chili, C93BO9)

Correspondence to: Dr. N. Mayer-Gostan (Tel.: +33-04-92-07-68-55; Fax: +33-04-92-07-68-50; E-mail: mayer@unice.fr)

the endolymph. Another feature of fish saccular endolymph is its high content of total CO_2 (Mugiya and Takahashi 1985). Biomineralization by formation of $CaCO_3$ on the otolith shifts the carbonic acid equilibrium towards acid values (Cameron 1990). The observation that endolymph fluid is more alkaline than plasma suggests that H^+ ions are pumped out by the epithelium and, if the potential measured by Enger (1964) is correct, this ion is not in electrochemical equilibrium. Thus, at least for K^+ and H^+, energy-dependent mechanisms appear to maintain gradients between the plasma and endolymph.

In most epithelia, active ion transport takes place in specialized cells, viz. ionocytes. In the mammalian inner ear, cells of the cochlear stria vascularis and vestibular dark cells are considered to be sites of endolymph production (Sterkers et al. 1988); they are rich in mitochondria and have a well-developed membrano-tubular system in which Na^+, K^+-ATPase is located, characteristics that are typical of ionocytes. Ionocytes have not been observed in the saccule of mammals (Kimura 1969). Studies of the morphology of the inner ear in fish mostly deal with sensory structures (Popper 1977, 1979) or the otolithic membrane (Dunkelberger et al. 1980). However, in a recent study, Becerra and Anadon (1993) have studied the structure and development of ionocyte-rich areas in the trout labyrinth and have found them exclusively in the wall of the utricle and crus commune and in the semicircular canal ampullae; they make no mention of any ionocyte-containing area in the saccular membranes.

We have therefore examined the saccule by use of coloration or probes known to characterize ion-transporting cells, in two species belonging to different orders, the fresh-water trout (*Oncorhynchus mykiss* – salmoniform) and the sea-water turbot (*Scophthalmus maximus* – pleuronectiform). Zinc iodide/osmium (ZIO) fixation is known to colour ionocytes (also called chloride cells) in fish gill (Avella et al. 1987; Mayer-Gostan et al. 1987; Madsen 1990; Watrin and Mayer-Gostan 1996) and has thus been used to detect the presence of cells that might react in the same manner as gill ionocytes. The saccular tissue has also been incubated with the isomeric styryl fluorescent dye dimethylaminostyrylmethylpyridiniumiodine (DASPMI; Bereiter-Hahn 1976; Mayer-Gostan et al. 1987) in order to visualize mitochondria-rich cells. Moreover, the localization of Na^+, K^+-ATPase in the saccular epithelium has been studied, as this enzyme has been shown to be more abundant in fish gill ionocytes than in pavement cells (Karnaky et al. 1976; McCormick 1990). Carbonic anhydrase has been immunolocalized because gill ionocytes have been shown to contain this enzyme (Lacy 1983; Rahim et al. 1988) and because this enzyme has been measured in the fish saccule (Mugiya et al. 1979). Intracellular acidic vesicles have been visualized by use of the weak base (Anderson and Orci 1988) acridine orange (AO), an amine that accumulates in acidic compartments of cells in living tissues. All observations have been performed either on whole tissue without embedding or on serial sections after embedding.

Materials and methods

Fish handling

Trout *(Oncorhynchus mykiss)* of about 200 g body weight were routinely collected from a local fish farm near Nice and reared in running tap water at about 14°C in circular tanks. Turbot *(Scophthalmus maximus)*, with a weight of 100–150 g, were obtained from facilities at IFREMER (Institut Français de Recherche pour l'Exploitation de la MER, Brest, France), flown to Nice and kept in a closed circuit of Mediterranean sea-water maintained at 16°C. The light in the aquarium room was on constantly for 12 h a day. Both groups were fed once a day, in the morning. The experiments reported in this article complied with the "Principles of animal care" of the National Institute of Health (publication no. 86–23, revised 1985) and the French laws for experiments on animals (décret no. 87–848).

Tissue sampling and preparation

Each fish was killed by rapid spinal section (less than 1 min) and decapitated behind the gills. The head was placed on ice and the skull opened by an antero-postero tangential cut and a dorsal cut just above the eyes. After anterior retraction of the brain, the ear was exposed and the semicircular canals and nerve branches were cut. The hemi-labyrinth was excised and either dropped into fixative (ZIO, Bouin's fixative or paraformaldehyde) or kept in an aerated modified Ringer's solution to be further dissected. The time between decapitation and tissue sampling was less than 2 min.

The ZIO fixative solution was prepared as previously described (Maillet 1959). Briefly, a filtered zinc iodide solution (ZnI_2) was prepared just before use (4.25 g zinc powder in 50 ml distilled water to which 1.25 g bisublimed iodine was added) and 4 parts of this solution were mixed at the last moment with 1 part of a 2% aqueous solution of osmium tetroxide. After fixation for 2–4 h at 4°C, tissue samples were rinsed in distilled water and either directly observed or dehydrated and embedded in Spurr resin (Fullam, Lathan, N.Y., USA). For direct observation, the hemi-labyrinth was either observed with a stereomicroscope or dissected as described below for living tissue and observed with a standard microscope (Polyvar, Reichert). For serial observations, ordered sections (0.5–2.0 μm, cut on an Ultracut E microtome, Reichert-Jung) of the tissue embedded in Spurr were glued on glass slides and observed with a light microscope.

Immunocytochemical detection of carbonic anhydrase II

Labyrinths were fixed with Bouin's fixative, rinsed with phosphate-buffer (PBS) but not embedded. After removal of the lagena, the opened saccule was incubated first with PBS containing 4% bovine serum albumin (PBS-BSA), then overnight at 4°C with the IgG fraction of a sheep polyclonal antiserum raised against human carbonic anhydrase II (The Binding Site, Birmingham, England) at a dilution of 1:1500 or with normal sheep serum (Jackson, West Grove, Pa., USA), rinsed with PBS-BSA and incubated for 3–4 h at room temperature with rabbit anti-sheep IgG (Jackson) at a dilution of 1:1000. After another rinse with PBS-BSA, the tissue was incubated with fluorescein-conjugated swine immunoglobulins to rabbit immunoglobulins (Dako, Trappes, France) at a dilution of 1:30 at room temperature for 2–3 h. The saccule was then rinsed with PBS, further dissected (as described below for living tissue observations), flattened on a glass slide and observed with an inverted fluorescence microscope (Olympus IMT 2). As the fluorescein isothiocyanate (FITC) fluorescent signal (excitation 488 nm, emission 520 nm) was low, a videocamera (Hamamatsu with image enhancer, Argus 20) was used. Images taken with the videocamera were continuously accumulated in the mem-

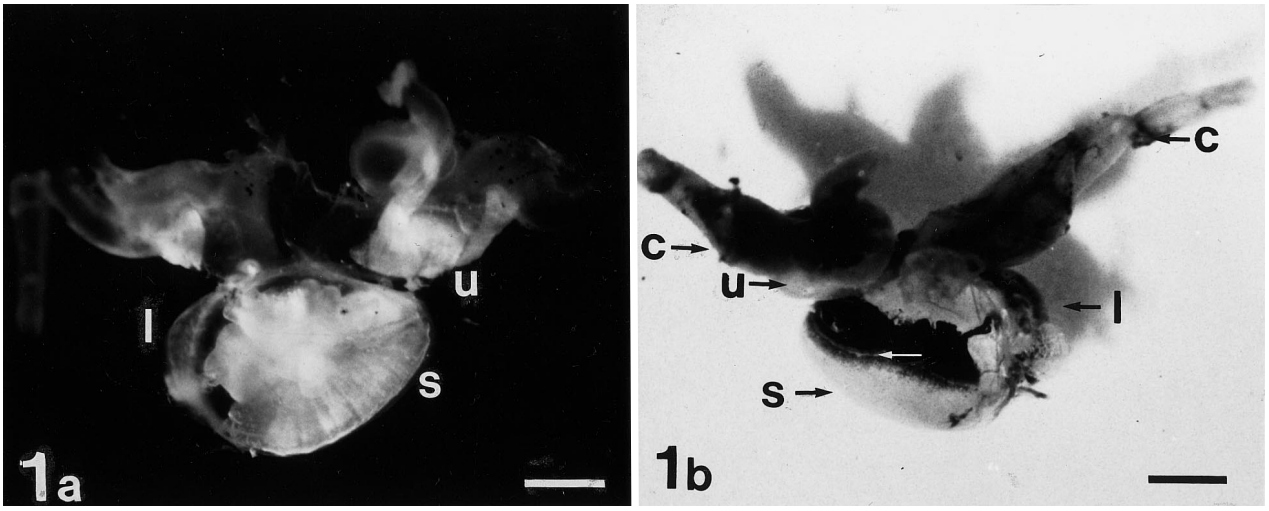

Fig. 1a, b. The membranous labyrinth of trout (*Oncorhynchus mykiss*) observed with the stereomicroscope. **a** Direct observation after excision; the position of the saccular otolith can be seen inside the saccule. ×7, *Bar:* 1.4 mm. **b** Zinc iodide/osmium (ZIO) fixation-coloration. A clear line (*white arrow*) separates the macula from another black area. ×6, *Bar:* 1.6 mm. *s*, Saccule; *l*, lagena; *u*, utricle; *c*, partially cut semicircular canals

ory and the accumulated image was displayed. This substantially improved the signal/noise ratio of the image.

Preparation of living tissue

Excised tissue was kept in aerated Ringer's solution until used. Dissection was visualized through a stereomicroscope and the tissue oriented with the saccular macula as a reference area. A ring-shape was first obtained by making two lateral circular cuts with ophthalmological scissors perpendicular to the long axis of the macula, thus making two symmetrical portions of a sphere that could be removed, one corresponding to the lagena. The ring was opened by a median cut through the macula. The piece of tissue was unfolded and flattened as much as possible on a glass slide with the endolymph side up. A small Cunningham perfusion chamber of about 100 µl was made and solutions were introduced and removed from the chamber as required. The incubation medium contained 135 mM NaCl, 1.5 mM $CaCl_2$, 1 mM $MgCl_2$, 0.4 mM KH_2PO_4, 5 mM $NaHCO_3$, 1 g/l glucose; the pH was adjusted to 7.4 with HCl and the solution was gassed with air before use. The probes DASPMI, AO and anthroyl-ouabain (all from Sigma-Aldrich Chimie, Saint Quentin Fallavier, France) were added to the incubation solution to give a final concentration of, respectively, 10, 3 and 5 µM. The freshly excised epithelium was exposed to the probe-containing medium for about 10 min for DASPMI and AO, and for 1 h for anthroyl-ouabain.To confirm that the fluorescent granules stained with AO were acidic vesicles, the disappearance of the orange fluorescence of the granules was checked after perfusion with ammonium chloride (10 mM), an agent that probably abolishes any proton gradient between the granules and cytoplasm. For DASPMI and AO, a band pass filter (450–480 nm) was used for excitation, with a 500-nm chromatic beam splitter and a 515-nm pass filter for emission, on a fluorescence microscope (Olympus IMT2). In the case of anthroyl-ouabain, the excitation beam was filtered through an interference filter (360 nm), whereas the emission was selected with a 420 nm filter. The images were viewed by a camera (Extended Isis, Photonic Science) with a sensitivity to 10^{-6} lx and the video signal processed (processor card DT 2867; Data translation, Marlboro, USA) in a PC (P 5/100 – Gateway 2000 Europe, Dublin Ireland). Image analysis was carried out with Axon software (Axon Imaging Worbench AIW, Calif., USA).

Results

Distribution of ZIO-positive cells in the hemi-labyrinth, particularly the saccule

The complete hemi-labyrinth of the trout before and after ZIO fixation-coloration and without dissection is shown in Fig. 1. The various chambers (utricle, saccule, lagena, canals) of the membranous labyrinth can be recognized and the otolith can be seen (Fig. 1a). After ZIO treatment (Fig. 1b), the nervous tissue and cut nerves appear black, allowing the recognition of the saccular macula; a black area can be distinguished almost completely enclosing the macula but is separated from the macula by a narrow clearer line.

After dissection of the saccule and observation from the endolymphatic side, the limit between the macula and the area of ZIO-positive cells can be clearly observed (Fig. 2a). These cells are organized as a meshwork near the long axis of the macula. Most cells appear to be connected to each other and their number decreases further from the macula where there are only a few isolated cells. Numerous capillaries are present in the connective tissue, which surrounds the meshwork of ZIO-stained cells.

In the portion of sphere roughly opposite to the macula, ZIO-positive cells were observed grouped in patches (Fig. 2b). They were different from those next to the macula as the cells were smaller and their ZIO-staining was not homogeneous, some cells being strongly positive, some being lightly coloured and others remaining uncoloured. Although patches were always observed, their number, position and size was difficult to analyse. An area with almost no ZIO-positive cells lay between the meshwork and the patches. Similar results were obtained in the saccule of turbot (not shown).

The saccular distribution of ZIO-positive cells in serial sections is presented in Fig. 3, with typical areas for

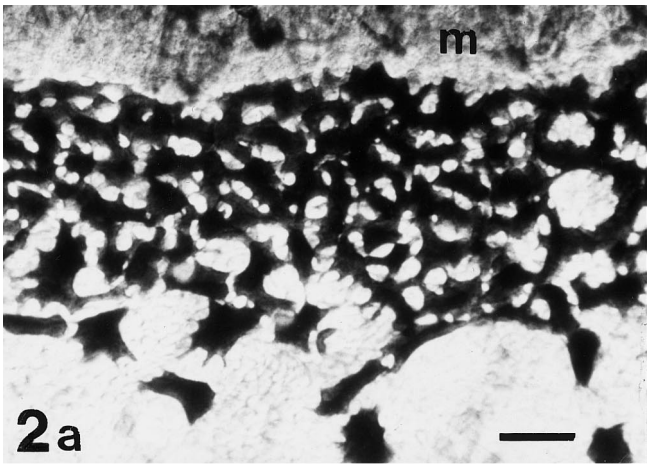

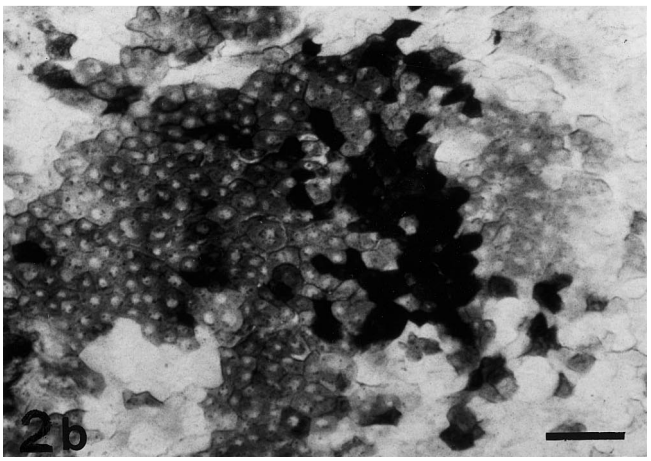

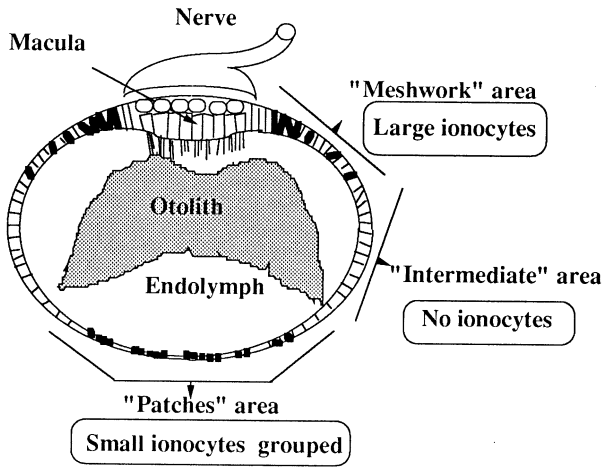

Fig. 2a, b. ZIO-fixed trout labyrinth; the dissected and flattened saccular tissue is viewed from the endolymphatic side. **a** Area near the macula. Note the clear separation between the macula (*m*) at the *top* and the ZIO-dark cells. The meshwork arrangement of the large ZIO-positive cells appears to be well separated from the macula. ×200, *Bar:* 50 μm. **b** Area opposite the macula. ZIO-stained small cells are grouped in patches. Note the different intensity in the black precipitate in the cells. ×200, *Bar:* 50 μm. **c** Line diagram of the saccular epithelium showing the localization of putative ionocytes

trout (Fig. 3a–d) and turbot (Fig. 3a′–d′). The saccular epithelium is surrounded by connective tissue of variable thickness. Estimations of the thickness of the connective tissue were only made for the trout (they were generally smaller in the turbot): about 70 μm near the macula (Fig. 3a) but only 40 μm at the opposite side (Fig. 3d). Blood vessels were observed in the connective tissue; the region next to the macula appeared to contain large numbers of blood vessels.

Four main regions of the saccular epithelium wall along a symmetrical axis crossing the macula can be distinguished as shown in Fig. 2c. (1) The macula is the nerve-containing region and has the greatest thickness (80–100 μm). The epithelium is stratified and fusiform ciliate cells in direct contact with the endolymph are lightly stained by ZIO (Fig. 3a, a′). (2) The "meshwork" area next to the macula (Fig. 3a, a′, b, b′) consists of an epithelium of 30–20 μm. Large ZIO-positive cells are separated from the macula by equally large cells that do not contain any precipitate. Although the epithelium appears to be stratified, the large ZIO-labelled cells cross the epithelium, their apical plasma membrane reaching the endolymphatic medium and their basal plasma membrane facing the connective tissue. Numerous capillaries irrigate this area. (3) The "intermediate" area between the "meshwork" and the "patches" areas is a region devoid of ZIO-positive cells. The thickness of the pseudostratified epithelium decreases progressively from 20 μm (Fig. 3c) near the "meshwork" area to 5 μm near the "patches" area and becomes a monolayer (Fig. 3c′). (4) The "patches" area lies opposite to the macula. The epithelium has a thickness of 6–9 μm and consists of a monolayer of cubical cells. Cells stained by ZIO (Fig. 3d, d′) occur in groups, the variable number of stained cells on successive sections suggesting patches.

The distribution of ZIO-positive cells in the saccule of trout and turbot is similar (Fig. 3). Minor differences mainly involve the thickness of the epithelium, which is particularly thin in the "intermediate" and "patches" areas of the turbot.

Mitochondria-rich cells in the saccular epithelium of trout

Observation on living fresh tissue after incubation with DASPMI showed that the macula was fluorescent, but

Fig. 3a–d. ZIO-fixed saccule of trout (*Oncorhynchus mykiss*). **a′–d′** ZIO-fixed saccule of turbot (*Scophthalmus maximus*). Serial sections. The typical areas are found successively from the macula to the opposite side. **a, a′** Macular area and beginning of the "meshwork" area with large ZIO-positive cells near the macula but separated from it by large non-labelled cells. **a** ×340, *Bar*: 30 μm. **a′** ×490, *Bar:* 20 μm. **b, b′** "Meshwork" area with large ZIO-dark cells; **b** and **b′** are in continuity with **a** and **a′**, respectively. **b** ×340, *Bar:* 30 μm. **b′** ×840, *Bar:* 12 μm. **c, c′** "Intermediate" area with no labelled cells; **c** is in continuity with **b**, whereas **c′** is near the "patches" area. **c** ×340, *Bar:* 30 μm. **c′** ×840, *Bar:* 12 μm. **d, d′** "Patches" area where small cells are labelled by ZIO. **d** ×270, *Bar:* 37 μm. *Insert:* ×840, *Bar:* 12 μm. **d′** ×840, Bar: 12 μm. *e*, Endolymph; *n*, nerve; *bv*, blood vessel; *m*, macula

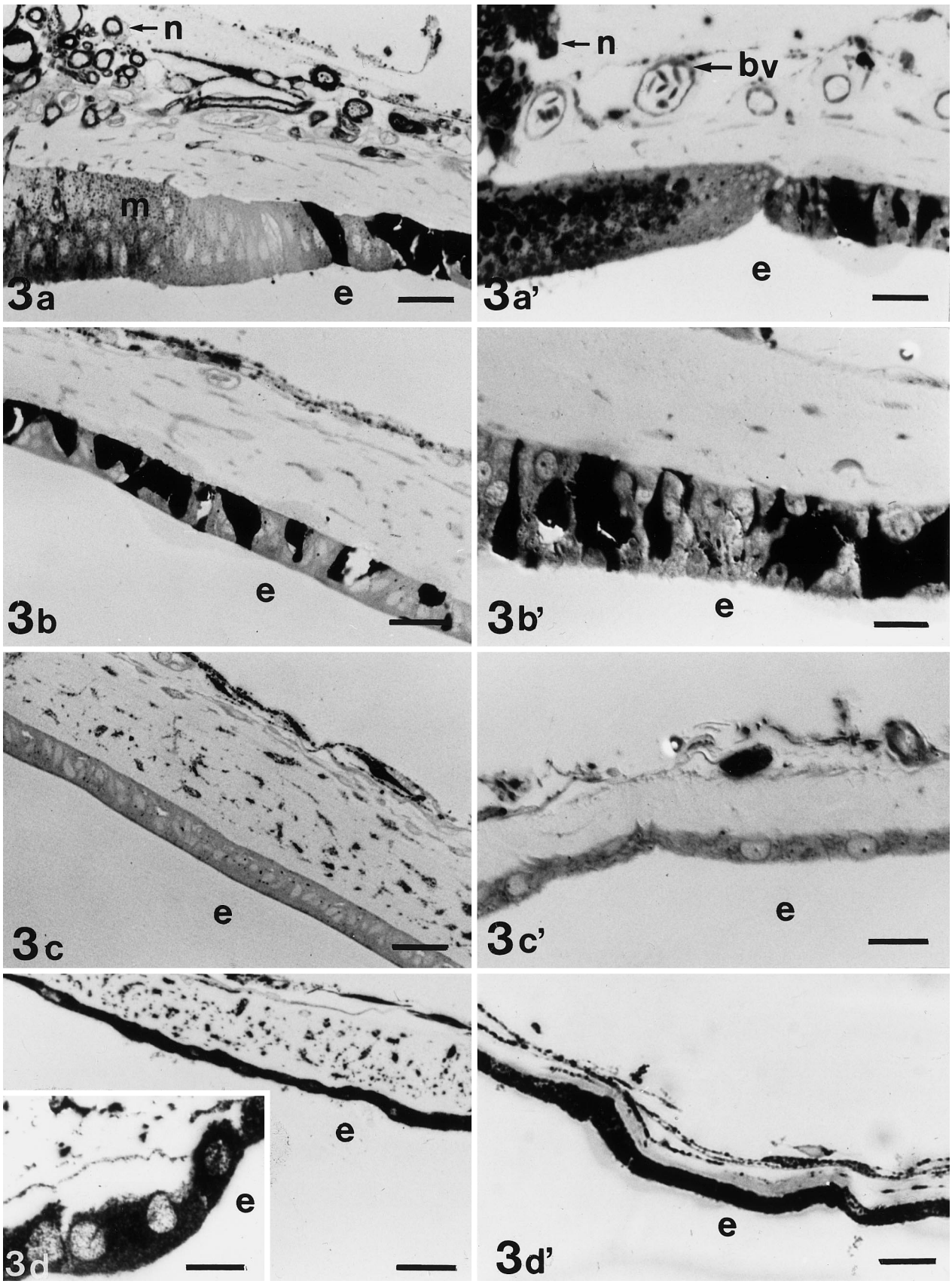
n
m
e
3a
n
bv
e
3a'
e
3b
e
3b'
e
3c
e
3c'
e
e
3d
e
3d'

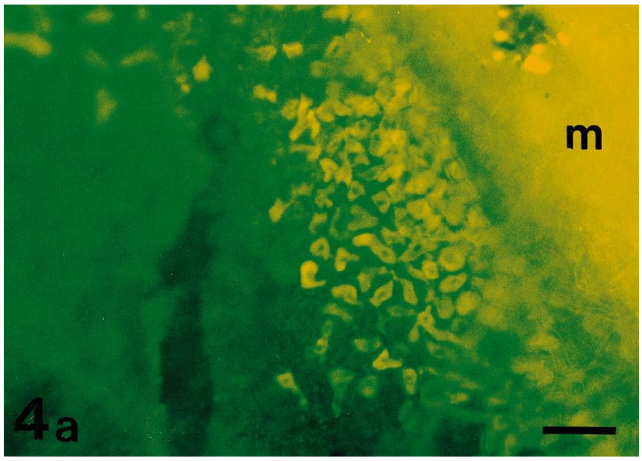

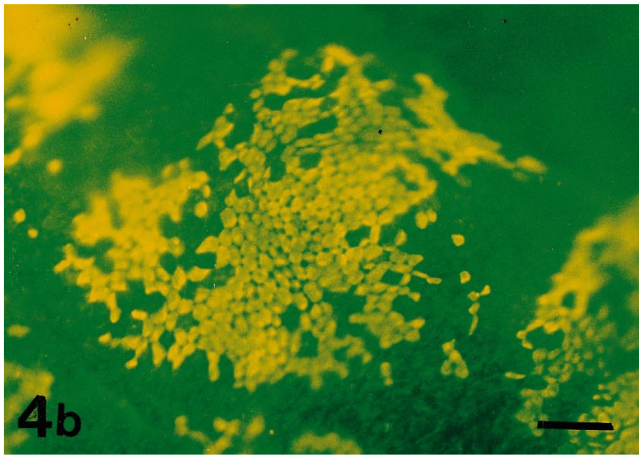

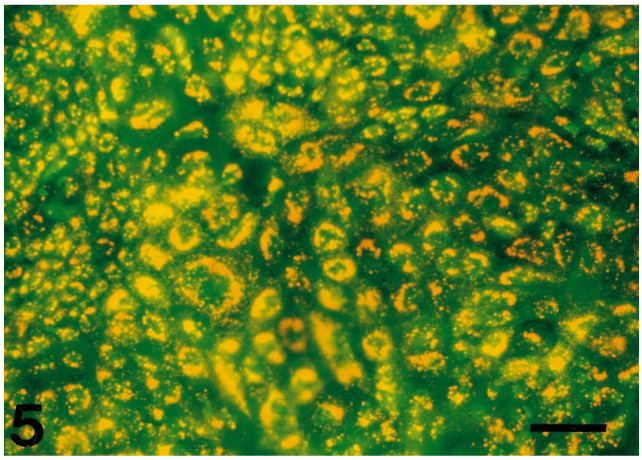

Fig. 4a, b. Observation of the living saccular epithelium of trout after incubation with the fluorescent mitochondrial probe DASPMI. **a** "Meshwork" area near the macula (*m*) and "intermediate" area. The fluorescent cells are large and organized into a meshwork similar to that in Fig. 2a, whereas the macula gives a general fluorescence. A part of the "intermediate" area appears green with no fluorescent cells. **b** "Patches" area opposite the macula. Note the patches of small DASPMI-positive cells. The thickness and infoldings of the tissue did not allow the whole field to be sharply focussed. ×100, *Bars:* 100 µm

Fig. 5. Acridine orange fluorescent staining of intracellular granules in the saccular epithelium of trout. The tissue includes the "intermediate" area and the "patches" area. The orange labelling of small intracytoplasmic vesicles is found throughout the epithelium, except in large cells of the "meshwork" area. Nuclei are stained green. ×190, *Bar:* 52 µm

the tissue thickness did not allow the fluorescent structures to be defined. The "meshwork" area could be recognized next to the macula where large cells, organized as a meshwork, were fluorescent (Fig. 4a). Smaller fluorescent cells were observed in the "patches" area, opposite to the macula (Fig. 4b) and, like the ZIO-positive cells in this area, they appeared to be grouped in patches. Differences in fluorescence intensity were observed between cells of this region; however, because the tissue was difficult to flatten, we could not conclude with certainty that this corresponded to variations in the amount of mitochondria. The "intermediate" area devoid of ZIO-positive cells was also devoid of DASPMI-fluorescent cells.

Cells labelled with anthroyl-ouabain in the saccular epithelium of trout

Observations on living tissue after incubation with anthroyl-ouabain showed two areas of fluorescent cells similar to those identified with ZIO and DASPMI. In the "meshwork" area next to the macula, large cells were organized as a network (data not shown). Smaller fluorescent cells were observed in the "patches" area, although their fluorescence was faint compared with that of cells observed in the "meshwork" area and they could be identified only because a highly sensitive videocamera was used.

Cells containing carbonic anhydrase II in the saccular epithelium of trout

Cells with cytoplasmic immunofluorescence were, likewise, observed in the two regions previously described as the "patches" and "meshwork" areas where ZIO-positive cells, DASPMI-fluorescent cells and anthroyl-ouabain fluorescent cells were seen (data not shown). The size of the cells and their organization (network of large cells in the "meshwork" area and groups of small cells in the "patches" area) were similar to those visualized by the other techniques.

Cells containing acidic vesicles in the saccular epithelium of trout

The nuclei of cells in fresh tissue incubated with AO showed a green fluorescence. Cells containing orange granules of variable sizes (generally small) were observed in nearly all the epithelium and were most obvious in the "patches" area opposite to the macula (Fig. 5). However, in contrast to all the previous labelling methods, the "meshwork" area was devoid of cells with orange granules. Exposure to ammonium chloride rapidly abolished the granular orange fluorescence, leaving only the green fluorescence of the nuclei, thus confirming the acidic nature of the granular structures.

A summary of the stainings observed in three of the main areas defined in the saccular epithelium is shown

Table 1. Summary of the staining of ionocytes in the saccular epithelium of trout and turbot (*ZIO*, zinc iodide/osmium; *DASPMI*, dimethylaminostyrylmethylpyridiniumiodine; *CAII*, carbonic anhydrase II; ++++, maximal staining; –, negative staining)

	"Meshwork" area	"Intermediate" area	"Patches" area
ZIO	++++	–	+++ or ++
DASPMI	++	–	++
Anthroyl-ouabain	++	–	+
CAII	++	–	+
Acridine orange	–	+	+

in Table 1. Staining observed in the macula area (mainly with ZIO and DASPMI) was not reported, because the cells stained could not be defined.

Discussion

In order to have as complete a view as possible of the whole epithelium, we have limited this study to observations with a stereomicroscope or light microscope. The ZIO procedure was originally developed for staining autonomic nerves (Maillet 1959) and for studies of synaptic vesicles. However, the biochemical significance of this staining is still not clear as it has been associated with many diverse factors, such as Ca^{2+}, ATP and –SH groups (Hayat 1993). To our knowledge, the ZIO fixation method has never before been used on the inner ear of any vertebrate. It produces dark staining not only of nerves, but also of epithelial cells. The clear distinction between the macula sensory cells and the adjacent epithelium could reflect a different embryological origin (the non-sensory structures arising from ectodermal epithelium). In the gill epithelium of teleosts, ZIO has been shown to stain chloride cells of fresh-water and sea-water fish (Garcia-Romeu and Masoni 1970; Avella et al. 1987; Madsen 1990; Watrin and Mayer-Gostan 1996). The strong black coloration of gill ionocytes after ZIO fixation permits their distinction from surrounding pavement cells and mucous cells. The number of gill cells stained by ZIO can be correlated with the magnitude of ion transport (Avella et al. 1987) and their proliferation as measured following hormonal treatment (Madsen 1990), which is known to modify ion exchange. In the saccule, ZIO has revealed two types of putative ionocytes: large cells in the area contiguous with the macula and patches of small cells that lie opposite to the macula and that stain with a wide range of intensities. The large cells share common features (a size of 20–30 μm, strong ZIO staining, contact with two different media) with the ionocytes observed in the gill or opercular membrane (Naon and Mayer-Gostan 1983, Avella et al. 1987; Karnaky 1986). The meshwork organization results from contacts between stained cells but cannot be described further at the magnifications used. The small ZIO-positive cells in the patches opposite to the macula do not differ in their shape from the surrounding pavement cells; however, they present a complex pattern with diversity in their strength of coloration and in their arrangement in patches. No fundamental differences have been observed between the primitive fresh-water trout and the more evolved pelagic sea-water turbot, at least as regards staining with ZIO. The bone opening in the turbot, which is smaller than the inner ear, and the fragility of the epithelium have not allowed us to test all the various probes in this species. Although only two species have been examined, we suspect that the presence of two types of ionocytes is a general feature of the fish saccule and is not related to environmental adaptation (depth of habitat or salinity) or to the degree of evolution but rather to some fundamental aspect of physiology (function of the macula and/or otolith depositions). However, ZIO staining alone, although shown to colour ion-transporting cells in various epithelia (Watrin and Mayer-Gostan 1996), is not sufficient to define the cells labelled in the saccule as ionocytes.

If one considers that richness in mitochondria is one of the best indicators of ionocytes, then the "patches" and "meshwork" regions that contain ZIO-positive cells (whatever the shape and size of the cells) must contain ionocytes, as DASPMI labels both areas. Gill and opercular ionocytes have been demonstrated with this probe (Mayer-Gostan et al. 1987; McCormick 1990). Ionocytes in structures other than the saccule in the fish inner ear have been characterized by their richness in mitochondria when examined electron-microscopically (Becerra and Anadon 1993) but, to our knowledge, this is the first time that DASPMI has been used on the inner ear of fish or in higher vertebrates.

Na^+, K^+-ATPase has been observed in the secretory dark cells of the vestibular tissue of the squirrel monkey and guinea-pig (Yoshihara et al. 1987; Ichimiya et al. 1994) and in the frog saccule (Burnham and Sterling 1984). The activity of the Na^+, K^+-ATPase measured in the ionocytes of fish gills has been shown to be 5 times greater than that in the respiratory cells (Naon and Mayer-Gostan 1983). The basolateral tubular system in the ionocytes of the fish gill is very rich in this enzyme (Karnaky et al. 1976) and, although anthroyl-ouabain has been shown to localize Na^+, K^+-ATPase in the ionocytes of the gill of teleost (McCormick 1990), it has not previously been used to localize this enzyme in the inner ear of fish. Despite there being no direct evidence that the labelled cells observed in our experiments are those stained by ZIO or those fluorescent after DASPMI, the similarities in location and shape are strong arguments for their identity as ionocytes.

Carbonic anhydrase II has been immunolocalized in the cytoplasm of cells that are ionocytes as judged by their localization in areas in which ZIO- and DASPMI-labelled cells are found. The low level of fluorescence could result from the loss of enzyme during the procedure and/or from the antibody having been raised against human carbonic anhydrase II. The presence of carbonic anhydrase is a feature shared with ionocytes of the gill (Lacy 1983; Rahim et al. 1988). Carbonic anhydrase activity has been demonstrated in the inner ear of cat (Erulkar and Maren 1961) and in the saccule of rainbow trout where its involvement in carbonate deposition in

the otolith has been proposed (Mugiya et al. 1979). The presence of carbonic anhydrase in the labyrinth of higher vertebrates is more controversial (Lim et al. 1983; Watanabe et Ogawa 1984). It has been observed or measured in the secretory area where vestibular dark cells are numerous but Ichimiya et al. (1994) have recently been unable to detect this enzyme in the vestibular dark cells of the guinea-pig. Our study has not necessarily detected all the cells that contain carbonic anhydrase, as it has many isoforms (Brechue et al. 1991). If it is confirmed that only certain cells contain this enzyme, their position could support the proposition that these cells contribute to creating, in the endolymph, a pH gradient that is important for otolith formation (Gauldie and Nelson 1990; Gauldie et al. 1995).

AO has been used to localize acidic compartments in various tissues and cells (Robbins and Marcus 1963, Maggio et al. 1990). Although the mechanism by which AO signifies a pH gradient is not yet clearly understood and its use for quantitative measurement of the amount of H^+ pumped has been questioned (Palmgren 1991), the present study shows that the dye does not accumulate in all the cells of the saccular epithelium. The "meshwork" area where large mitochondria-rich cells have been observed is completely devoid of staining. There appears to be no previous study of the distribution of this dye in the inner ear epithelium and it will be necessary to use other pH probes or immunostaining of enzymes (e.g. H^+-ATPase) to show whether there are two distinct types of ionocytes.

In conclusion, the saccule has specialized cells that have all the characteristics of ionocytes. This suggests that endolymph production in the saccule does not depend on the ionocytes in the semicircular canal ampullae, crus commune or utricle (Becerra and Anadon 1993), irrespective of whether the saccule communicates with other chambers. The present work suggests the presence of two types of ionocytes having different functions (e.g. K^+ secretion, water exchange, Ca^{2+} and H^+ exchanges), although further experiments are necessary to confirm this. The trout saccule, which can be easily dissected out, provides a useful model for investigating ion and water exchange mechanisms in the inner ear.

Acknowledgments. We are grateful to Professor J. F. Morris for his comments, suggestions and corrections, particularly with respect to language.

References

Anderson RGW, Orci L (1988) A view of acidic intracellular compartments. J Cell Biol 106:539–543

Avella M, Masoni A, Bornancin M, Mayer-Gostan N (1987) Gill morphology and sodium influx in the rainbow trout (*Salmo gairdneri*) acclimated to artificial environments. J Exp Zool 241:159–169

Becerra M, Anadon R (1993) Fine structure and development of ionocyte areas in the labyrinth of the trout (*Salmo trutta fario*). J Anat 183:463–474

Bereiter-Hahn J (1976) Dimethylaminostyrylmethylpyridiniumiodine (DASPMI) as a fluorescent probe for mitochondria in situ. Biochim Biophys Acta 423:1–14

Brechue WF, Kinne-Saffran E, Kinne RKH, Maren TH (1991) Localization and activity of renal carbonic anhydrase (CA) in CA-II deficient mice. Biochim Biophys Acta 1066:201–207

Burnham JA, Sterling CE (1984) Quantitative localization of Na-K pump site in the frog sacculus. J Neurocytol 13:617–638

Campana SE, Neilson JD (1985) Microstructure of fish otoliths. Can J Fish Aquat Sci 42:1014–1032

Cameron JN (1990) Unusual aspects of calcium metabolism in aquatic animals. Annu Rev Physiol 52:77–95

Dale T (1980) Surface morphology of the acoustico-lateralis sensory organ in teleosts: functional and evolutionary aspects. In: Ali MA (ed) Environmental physiology of fishes. Plenum, New York London, pp 387–402

Dunkelberger DG, Dean JM, Watabe N (1980) The ultrastructure of the otolithic membrane and otolith in the juvenile mummichog, *Fundulus heteroclitus*. J Morphol 163:367–377

Enger PR (1964) Ionic composition of the cranial and labyrinthine fluids and saccular DC potentials in fish. Comp Biochem Physiol 11:131–137

Erulkar SD, Maren TH (1961) Carbonic anhydrase and the inner ear. Nature 189:459–460

Fänge R, Larsson A, Lidman U (1972) Fluids and jellies of the acusticolateralis system in relation to body fluids in *Coryphaenoides rupestris* and other fishes. Mar Biol 17:180–185

Garcia-Romeu F, Masoni A (1970) Sur la mise en évidence des cellules à chlorure de la branchie de poissons. Arch Anat Micro Exp 59:289–294

Gauldie RW, Nelson DGA (1990) Otolith growth in fishes. Comp Biochem Physiol 97A:119–135

Gauldie RW, West IF, Coote GE (1995) Evaluating otolith age estimates for *Hoplostethus atlanticus* by comparing patterns of checks, cycle in microincrement width, and cycles in strontium and calcium composition. Bull Mar Sci 56:76–102

Hayat MA (1993) Stains and cytochemical methods. Plenum, New York London

Ichimiya I, Adams JC, Kimura RS (1994) Immunolocalization of Na^+,K^+-ATPase, Ca^{++}-ATPase, calcium-binding proteins, and carbonic anhydrase in the guinea pig inner ear. Acta Otolaryngol 114:167–176

Jones CM (1992) Development and application of the otolith increment technique. In: Stevenson DK, Campana SE (eds) Otolithic microstructure examination and analysis. Canadian Special Publication of Fish Aquatic Science, no. 117, pp 1–11

Kalish JM (1991) Determinants of otolith chemistry: seasonal variation in the composition of blood plasma, endolymph and otoliths of bearded rock cod *Pseudophycis barbatus*. Mar Ecol Prog Ser 74:137–159

Karnaky KJ (1986) Structure and function of the chloride cells of *Fundulus heteroclitus* and other teleosts. Am Zool 26:209–224

Karnaky KJ, Kinter LB, Kinter WB, Stirling CE (1976) Teleost chloride cells. II. Autoradiographic localization of gill Na, KATPase in killifish *Fundulus heteroclitus* adapted to low and high salinity environments. J Cell Biol 70:157–177

Kimura RS (1969) Distribution, structure and function of dark cells in the vestibular labyrinth. Ann Otol Rhynol Laryngol 78:542–561

Lacy ER (1983) Histochemical and biochemical studies of carbonic anhydrase activity in the opercular epithelium of the euryhaline teleost, *Fundulus heteroclitus*. Am J Anat 166:19–39

Lim DJ, Karabinas C, Wersall J (1983) Histochemical localization of carbonic anhydrase in the inner ear. Am J Otolaryngol 4:33–42

Lowenstein O (1971) The labyrinth. Fish Physiol 5:207–240

Madsen SS (1990) The role of cortisol and growth hormone in seawater adaptation and development of hypoosmoregulatory mechanisms in sea trout parr (*Salmo trutta*). Gen Comp Endocrinol 79:1–11

Maggio K, Keicher E, Hernandez-Nicaise ML, Gillot I, Nicaise G (1990) Quenching of proton gradient and concomitant in-

crease of intragranular calcium in interstitial cells of *Mytilus* retractor muscle. Cell Tissue Res 262:149–156

Maillet M (1959) Modification de la technique de Champy au tetroxyde d'osmium-iodure de potassium. Résultats de son application à l'étude des fibres nerveuses. C R Seance Soc Biol Fil 153:939–940

Mayer-Gostan N, Wendelaar Bonga SE, Balm PHM (1987) Mechanisms of hormone actions on gill transport. In: Pang PKT, Schreibman MP (eds) Vertebrate endocrinology: fundamentals and biomedical implications, vol 2. Academic Press, San Diego, pp 211–238

McCormick SD (1990) Fluorescent labelling of Na^+,K^+-ATPase in intact cells by use of a fluorescent derivative of ouabain: salinity and teleost chloride cells. Cell Tissue Res 260:529–533

Morgon A, Aran JM, Collet L, Dauman R, Fraysse B, Freyss G, Pujol R, Sens A, Sterkers O, Tran Ba Huy P, Uziel A eds. Societé Française d'Oto-Rhino-Laryngologie et de Pathologie Cervico-Faciale. Arnette S.A. Paris (1990) Données actuelles sur la physiologie et la pathologie de l'oreille interne. In: Arnette (ed) Soc Française d'Oto-Rhino-Laryngologie et de Pathologie Cervico-Faciale, Paris

Mugiya Y, Takahashi K (1985) Chemical properties of the saccular endolymph in the rainbow trout, *Salmo gairdneri.* Bull Fac Fish Hokkaido Univ 36:57–63

Mugiya Y, Kawamura H, Aratsu S (1979) Carbonic anhydrase and otolith formation in the rainbow trout, *Salmo gairdneri* : enzyme activity of the sacculus and calcium uptake by the otolith in vitro. Bull Jpn Soc Sci Fish 45: 879–882

Naon R, Mayer-Gostan N (1983) Separation by velocity sedimentation of the gill epithelium cells and their ATPase activities in the seawater adapted eel, *Anguilla anguilla* L. Comp Biochem Physiol 75A: 541–547

Palmgren MG (1991) Acridine orange as a probe for measuring pH gradients across membranes: mechanisms and limitations. Anal Biochem 192:316–321

Panella G (1971) Fish otoliths: daily growth layers and periodical patterns. Science 173:1124–1127

Popper AN (1977) A scanning electron microscopic study of the sacculus and lagena in the ears of fifteen species of teleost fishes. J Morphol 153: 397–418

Popper AN (1979) Ultrastructure of the sacculus and lagena in a moray eel (*Gymnothorax* sp.). J Morphol 161: 241–256

Rahim SM, Delaunoy JP, Laurent P (1988) Identification and immunocytochemical localization of two different carbonic anhydrase isoenzymes in teleostean fish erythrocytes and gill epithelia. Histochemistry 89:451–459

Robbins E, Marcus PI (1963) Dynamics of acridine orange-cell interaction. I. Interrelationships of acridine orange particles and cytoplasmic reddening. J Cell Biol 18:237–250

Sterkers O, Ferrary E, Amiel C (1988) Production of inner ear fluids. Physiol Rev 68: 1083–1128

Sterkers O, Tran Battuy P, Ferrari E (1990) Physiologie des liquides de Koreille Interne p 93–135 in: "Donmées actuelles sur la physiologie et la pathologie de Koreille interne

Watanabe Y, Miyamoto H (1973) Biochemistry study of labyrinthine fluids (of the fish). Med J Osaka Univ 23:273–282

Watanabe K, Ogawa A (1984) Carbonic anhydrase activity in stria vascularis and dark cells in vestibular labyrinth. Ann Otol Rhynol Laryngol 93:262–266

Watrin A, Mayer-Gostan N (1996) Simultaneous recognition of ionocytes and mucus cells in the gill epithelium of turbot and in rat stomach. J Exp Zool 275

Yoshihara T, Usani S, Igarashi M, Fermin CD (1987) Ultracytochemical study of ouabain-sensitive, potassium-dependent p-nitrophenyl phosphatase activity in the inner ear of the squirrel monkey. Acta Otolaryngol 103:161–169